

See discussions, stats, and author profiles for this publication at: <https://www.researchgate.net/publication/235366185>

Refined Magic–Angle Coil Spinning Resonator for Nanoliter MAS NMR Spectroscopy: Enhanced Spectral Resolution.

ARTICLE *in* ANALYTICAL CHEMISTRY · JANUARY 2013

Impact Factor: 5.64 · DOI: 10.1021/ac400188b · Source: PubMed

CITATIONS

8

READS

31

3 AUTHORS, INCLUDING:



[Alan Wong](#)

French National Centre for Scientific Research

65 PUBLICATIONS 1,401 CITATIONS

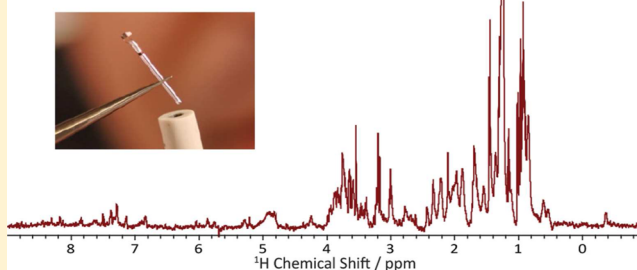
SEE PROFILE

Refined Magic-Angle Coil Spinning Resonator for Nanoliter NMR Spectroscopy: Enhanced Spectral Resolution

Alan Wong,^{*,†} Xiaonan Li,^{†,§} and Dimitris Sakellariou^{†,‡}[†]CEA Saclay, DSM, IRAMIS, UMR CEA/CNRS 3299 – SIS2M, Laboratoire Structure et Dynamique par Résonance Magnétique, F-91191, Gif-sur-Yvette Cedex, France[‡]Ecole Normale Supérieure, 24 rue Lhomond, F-75005 Paris, France

ABSTRACT: The magic-angle coil spinning (MACS) resonator allows a simple approach for nanoliter nuclear magnetic resonance (NMR) detections with enhanced sensitivity and high-resolution under sample magic-angle spinning (MAS). Currently, the spectral resolution acquired with MACS is not efficient for detailed characterization of semisolids like biopsies, where subhertz resolution is necessary. Here, we describe the two sources of line broadening from MACS, sample temperature gradient and anisotropic magnetic susceptibility, and present a refined high-resolution magic-angle coil spinning (HR-MACS) resonator that improves the spectral resolution. We demonstrate with the high quality HR-MACS NMR spectra of micronematodes and tissue biopsy, and illustrate its potential for NMR-based metabolomics of nanoliter tissue samples.

Nano-Liter NMR Biopsy



The recent developments on inductively coupled rotating-microcoil resonator known as magic-angle coil spinning (MACS)^{1,2} have shown great promises for nanovolume magic-angle spinning (MAS) nuclear magnetic resonance (NMR) detections of semisolid materials such as tissue biopsies.^{3,4} Besides the sensitivity enhancement, owing to the increase in magnetic field flux from the microsolenoidal coil, one other advantage is its excellent versatility. The MACS resonator can be readily coupled with any standard commercial MAS probe without the need for modification. Moreover, the fact that the sample is spun together with the resonator averages out the line broadening induced by the inhomogeneous isotropic magnetic susceptibility from the resonator and the sample. Recently, we have evaluated the performance of MACS for metabolic profiling of nanoliter biopsies of bovine muscle and human gastric mucosal tumor⁴ and found that the gain in sensitivity allows one to resolve metabolite resonances in a reasonable acquisition time span, presenting a potential prognostic and diagnostic tool for clinical studies of scarce biopsies. However, the resultant ¹H spectral resolution 5–10 Hz (at 11.75 T) from the MACS resonator is still rather insufficient for in-depth metabolic phenotyping. The resolution is in fact below today's standards of high-resolution (HR)-MAS NMR spectroscopy for biopsy studies.⁵ Therefore, the spectral resolution acquired with MACS must be improved in order to be applicable for metabolomics applications. In this short report, we describe the two contributions of line broadening from MACS detection and present a refined high-resolution MACS (HR-MACS) resonator that is capable of 1 Hz resolution. We demonstrate its superior spectral quality for nanoliter NMR detection of tissues.

■ METHODS

MACS Fabrication. Each MACS resonator was constructed by manually hand winding a 10-turns solenoidal coil from either a commercially available 62 or 30 μ m cross-section copper (Cu) round wire around a 550/400 μ m (outer/inner diameter) quartz capillary, forming a solenoidal length of 1.5–2.0 mm with a sample detection volume of about 188–250 nL. The solenoid was soldered to a nonmagnetic 3.0 or 3.3 pF capacitor (American Technical Ceramics, US), to give a target frequency at 500 ± 25 MHz for ¹H detection at 11.75 T. The resultant coil quality factors are in the range of 40–50.

Sample Preparation. Sample preparation for MACS was preformed under a microscope with microtools. For sucrose solution and *Caenorhabditis elegans* nematodes, the samples were pipetted directly into the solenoid region of the quartz capillary using a micropipet with a 20 μ L GELoader tip (Eppendorf, US). The capillary was then sealed with hot paraffin wax to prevent leakage during the sample spinning. Due to the slight adhesive texture of the tissue, the preparation of the kidney tissue involved multiple steps: (1) cutting a frozen microsize tissue and quickly submerging it into a D₂O saline solution; (2) using a microtweezers and placing the washed tissue inside the tip of the open-ended capillary; (3) securing the MACS in a custom-made cylindrical plastic insert and centrifuging at 14 500 rpm (about 60 s) until the tissue was displaced into the solenoid region; (4) filling the solenoid

Received: October 4, 2012

Accepted: January 23, 2013

Published: January 23, 2013

region with D₂O and sealing the capillary with hot wax; (5) securing the sample-filled MACS in a custom-made insert designed to fit tightly inside a commercial 4-mm ZrO Bruker rotor for coil protection and stability during spinning. To minimize the tissue degradation, the entire tissue preparation procedure was restricted to no longer than 10 min.

¹H NMR Spectroscopy. NMR experiments were carried out on a wide-bore Bruker Avance II spectrometer with a Bruker 4-mm HX CP-MAS probe. It should be mentioned that a commercial high-resolution (HR)-MAS probe⁶ would have provided the optimal sensitivity and resolution for ¹H detections, owing to the ¹H-optimized coil and the ability for external field locking during acquisitions, which is critical for long experiments. Unfortunately, our laboratory is not equipped with the HR-MAS probe; thus, the results here represent a slightly less than optimal condition. The shimming of the magnetic field was performed under sample spinning by monitoring the water or the sucrose resonances. Since the MAS rotor is placed on the plane of ZY shimming axis, the sample spinning rendered a simplified shimming procedure^{7,8} by mainly using the Z, Y, X2 – Y2, ZY, Z3, and Z(X2 – Y2) shims. The MAS frequency was controlled by a Bruker MAS pneumatic unit with ±1 Hz accuracy. A 2D-PASS sequence⁹ was applied to acquire sideband-free spectra for all MAS experiments with spinning frequencies below 1000 Hz. Water suppression was achieved using low-power irradiation on the water resonance during the recycle delay of 1 s.

RESULTS AND DISCUSSION

Figure 1 shows a typical spectral resolution difference from the detection of MACS and of CP-MAS with sample spinning at

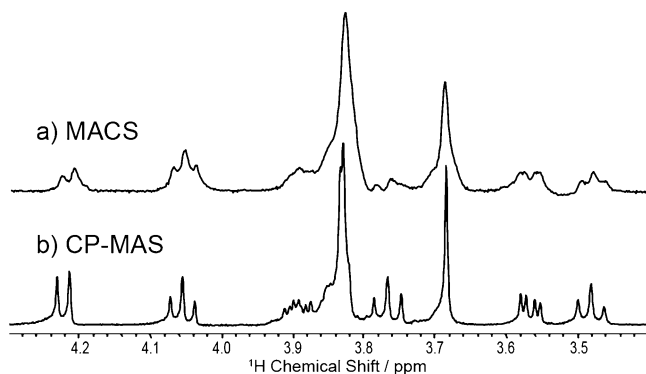


Figure 1. ¹H NMR spectral comparison of sucrose in H₂O displaying the differences in spectral resolution using (a) MACS and (b) CP-MAS detection. The spectra were acquired with 1500 Hz sample spinning, with sample detection volumes of about (a) 200 nL in a quartz capillary and (b) 30 μL in a MAS Kel-F bioinsert. Spectra are processed without apodization.

1500 Hz. The ¹H MACS spectrum of sucrose displays resonances that are substantially broader than that of CP-MAS. The obvious sources of the broadening are 2-fold: (i) the presence of sample temperature gradient originating from the eddy currents in the coil spinning and (ii) the presence of anisotropic magnetic susceptibility in the insert.

Sample Temperature Gradient. Like any standard MAS experiments, sample heating is an issue especially for sensitive samples such as biopsies. Friction-induced¹⁰ and radio frequency induced¹¹ heating are the main sources for fast MAS experiments. However, in the case of a coil spinning with

MACS, a different heating mechanism arises. The heating is induced by the eddy currents^{12,13} created within the conductive materials, which experience a variation in magnetic field flux as they are spun together with the MAS rotor inside the external static magnetic field. Such heating can create a temperature gradient along the sample region and subsequently lead to broadening caused by the frequency shift in resonance. For a water sample, the consequences can be quite severe since the ¹H chemical shift of HDO is strongly temperature dependent, −11.9 ppb/°C,¹⁴ in other words 5.95 Hz/°C at 11.75 T.

Sakellariou and co-workers^{12,13} have examined the eddy current effects in the spinning solenoidal coil in a magnetic field. The authors have formulated the dissipated power *P* generated by the eddy currents in a coil that spins at magic-angle (54.74°) to a homogeneous magnetic field and found that *P* has a strong dependence to the coil spinning frequency ($\omega_r = 2\pi\nu_r$), coil radius, and the cross-section of the wire. Increasing any of these factors would lead to an increase in the power dissipation and, thus, an increase in sample heating. It has previously reported¹² that a solenoidal coil constructed with 62 μm cross-section Cu wire, spinning at 6000 Hz inside a 11.75 T magnet, results in heating the sample by 37 °C, whereas the heating decreases to 1.6 °C with a 25 μm Cu wire. This would further decrease to no more than 0.02 °C if the coil spinning is reduced to 500 Hz. The spectral comparison between Figure 2a,b clearly shows an improvement in resolution, better J-splitting with narrower lines, using smaller cross-section Cu wire, 30 μm instead of 62 μm, and with slower MAS acquisition, 336 Hz instead of 1500 Hz. Since the dense patterns of spinning sidebands arise in the spectra under slow MAS condition, a spinning-sidebands suppression experiment 2D-PASS (phase-adjust spinning sidebands)⁹ is applied to give the isotropic spectra. 2D-PASS is a rotor-synchronized experiment that averages out the sidebands by manipulating the phases of the sideband signals. It requires a rotor period to record the sideband-free isotropic spectra. This rotor-synchronization can also provide a T₂-filter mechanism for suppressing macromolecule NMR resonances in tissues. This is similar to the relaxation-edited CPMG-T₂-filter experiment,⁵ which is often applied to filter the lipid and protein resonances in biopsies.

Magnetic Susceptibility. One other source is the heterogeneous magnetic field from the sample local environments. The effect of this magnetic field induced line width can be described by $B_0 = \mu_0(1 + \chi_j)H_0$, where the magnetic field *B*₀ experienced by the nuclear spins is modified by the magnetic susceptibility χ of the local medium *j* under the external static magnetic field *H*₀. The χ_j , such as the Cu wire used in the MACS resonator and the insert for MACS, can create a heterogeneous *B*₀ field for the nuclear spins to resonate at a series of different resonance frequencies and result in broadening. This distribution of *B*₀ can be treated as a sum all the different magnetic dipoles between the nuclear spin and the medium. Under MAS, the time-dependent magnetic dipole field¹⁵ will average to zero and give rise to isotropic resonances with spinning sidebands, only if χ_j is isotropic, whereas if χ_j has anisotropic magnetic susceptibility, then the magnetic dipole field can no longer be completely averaged under MAS and results in residual line broadening. To illustrate this, Figure 2b shows that the spectral resolution has improved dramatically by minimizing the eddy current heating in the MACS resonator with small cross-section Cu wire under slow MAS; however, residual line broadening about 4–5 Hz is still clearly visible in

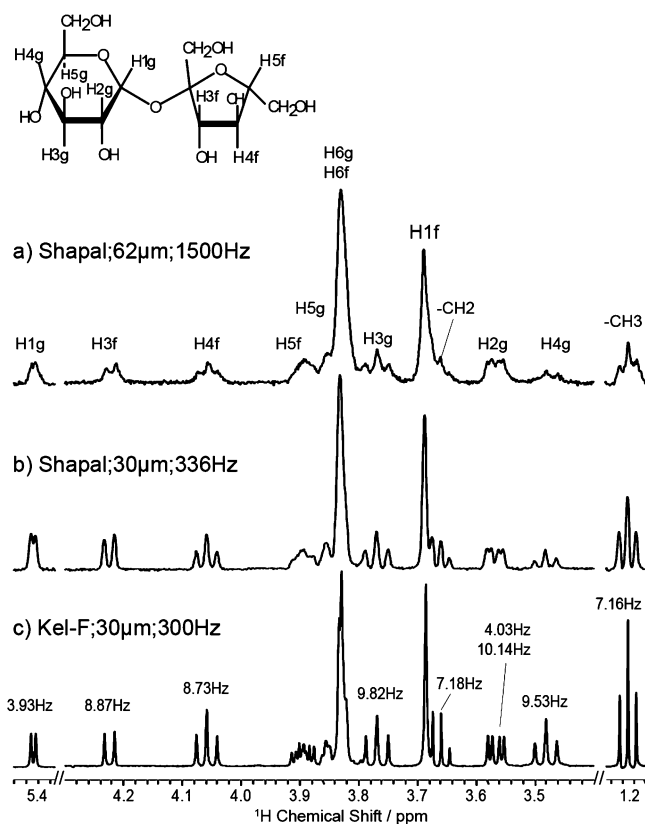


Figure 2. A ^1H NMR spectral comparison of ~ 200 nL sucrose/ethanol in H_2O displaying the resolution differences using different MACS configurations: (a) 62 μm Cu-wire solenoid with Shapal-M insert spinning at 1500 Hz; (b) 30 μm Cu-wire solenoid with Shapal-M insert spinning at 336 Hz; and (c) 30 μm Cu-wire solenoid with Kel-F insert spinning at 300 Hz. Spectra are processed with no apodization. A drop of ethanol is added to provide additional known J-splitting in the spectrum. The peak assignments correspond to the top inserted sucrose molecule, where g and f denote as the monosaccharide glucose and fructose, respectively. The peaks H1f, H6f, and H6g correspond to the $-\text{CH}_2-$ protons. Selective J-coupling values are indicated above the corresponding peaks in spectrum (c). The full-width at half-maximum for the H1f proton at 3.69 ppm are found to be (a) 6.6 Hz, (b) 3.9 Hz, and (c) 2.0 Hz.

the spectrum. This broadening is due to the anisotropic magnetic susceptibility¹⁵ of the ceramic Shapal-M (aluminum nitride) insert. Originally, the use of Shapal-M insert is designed to protect and stabilize the MACS resonator during spinning, owing to its good mechanical strength and excellent thermal conductivity for heat dissipation. However, the magnetic dipole between the sample and the anisotropic magnetic susceptibility of the Shapal-M cannot completely average to zero under MAS¹⁵ resulting in the observed residual broadening. To eliminate this anisotropic magnetic susceptibility effect, the Shapal-M insert is replaced with an isotropic magnetic susceptibility material Kel-F. This enables one to completely cancel the magnetic dipole field under MAS condition and results in less than 1 Hz line width resolution with well-defined J-splitting resonances (Figure 2c), including the H2g proton at 3.56 ppm, which is a doublet of doublets resonance with J-coupling values of 4.03 and 10.13 Hz. The small J-coupling is difficult to determine from the spectrum acquired with a nonrefined MACS resonator (Figure 2a). It should be noted that since the insert is in the MAS together with the resonator

and sample, it is unnecessary to use susceptibility-matched (or -compensated) materials for the insert because the MAS eliminates the susceptibility broadening as long as the materials have isotropic susceptibility.

Spinning of a HR-MACS Resonator. Since the magic-angle spinning of both the sample and the resonator is an important factor to high-resolution NMR spectroscopy, and the eddy currents in the spinning coil are dependent upon spinning frequency, it is important to experimentally evaluate the coil spinning effects on the line resolution. Figure 3 shows a well-

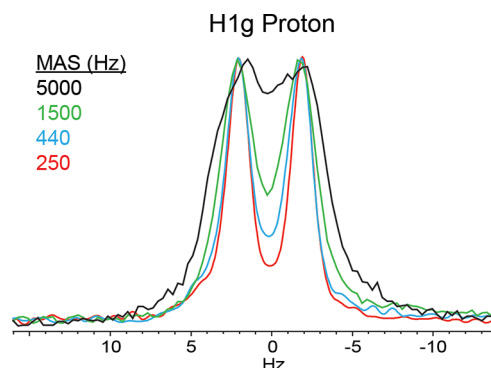


Figure 3. Doublet of an anomeric proton H1g in sucrose, acquired with HR-MACS at different MAS frequencies. It illustrates the loss of spectral resolution as the MAS frequency increases. Spectra are processed with no apodization.

defined doublet ($^3J_{\text{H-H}} = 3.97$ Hz with 81% splitting depth) of the sucrose anomeric proton resonance H1g. It is recorded with a HR-MACS resonator fitting inside a Kel-F insert spinning at a slow frequency of 250 Hz (Table 1). The resolution worsens as

Table 1. Summary of the Line Resolution Acquired with HR-MACS^a under Various MAS Frequency (See Figure 3)

MAS (± 1 Hz)	J-splitting depth ($\pm 1\%$)	FWMH ^b (± 0.02 Hz)	estimated P^c (nW)	estimated T_{inc}^d ($^{\circ}\text{C}$)
250	81	5.57	6.8	0.0004
440	70	5.65	21.4	0.01
1500	56	6.23	249	0.2
5000	~ 5	7.21	2800	1.8

^aThe HR-MACS resonator is constructed of a 550 μm diameter 10-turns solenoidal coil in 1.7 mm length with 30 μm Cu wire. ^bFWMH = full-width at half-maximum. ^cThe power dissipation is estimated using eq 11 in ref 13. ^dThe sample heating is estimated using thermal simulations performed with Quickfield described in ref 12.

the spinning increases. At 5000 Hz, the doublet is nearly not visible with a J-splitting depth of about 5%. To evaluate the temperature distributions along the sample, we adopted the mathematical model developed by Sakellariou and co-workers¹³ to estimate the power dissipations from the coil at different MAS frequencies and apply them for a thermal simulation of the sample temperature profile.¹² The results are tableted in Table 1. It is found that even though the HR-MACS resonator is in direct contact with the poorly thermally conductive Kel-F insert, the estimated power dissipation is small, less than 30 nW for MAS below 500 Hz. This results in a sample temperature heating with no more than 0.02 $^{\circ}\text{C}$; thus, the effect on line broadening is minimal. However, at rapid spinning of 5000 Hz, the power dissipation is largely increased to 2800 nW and leads to a significant sample heating of about 1.8 $^{\circ}\text{C}$ over the small

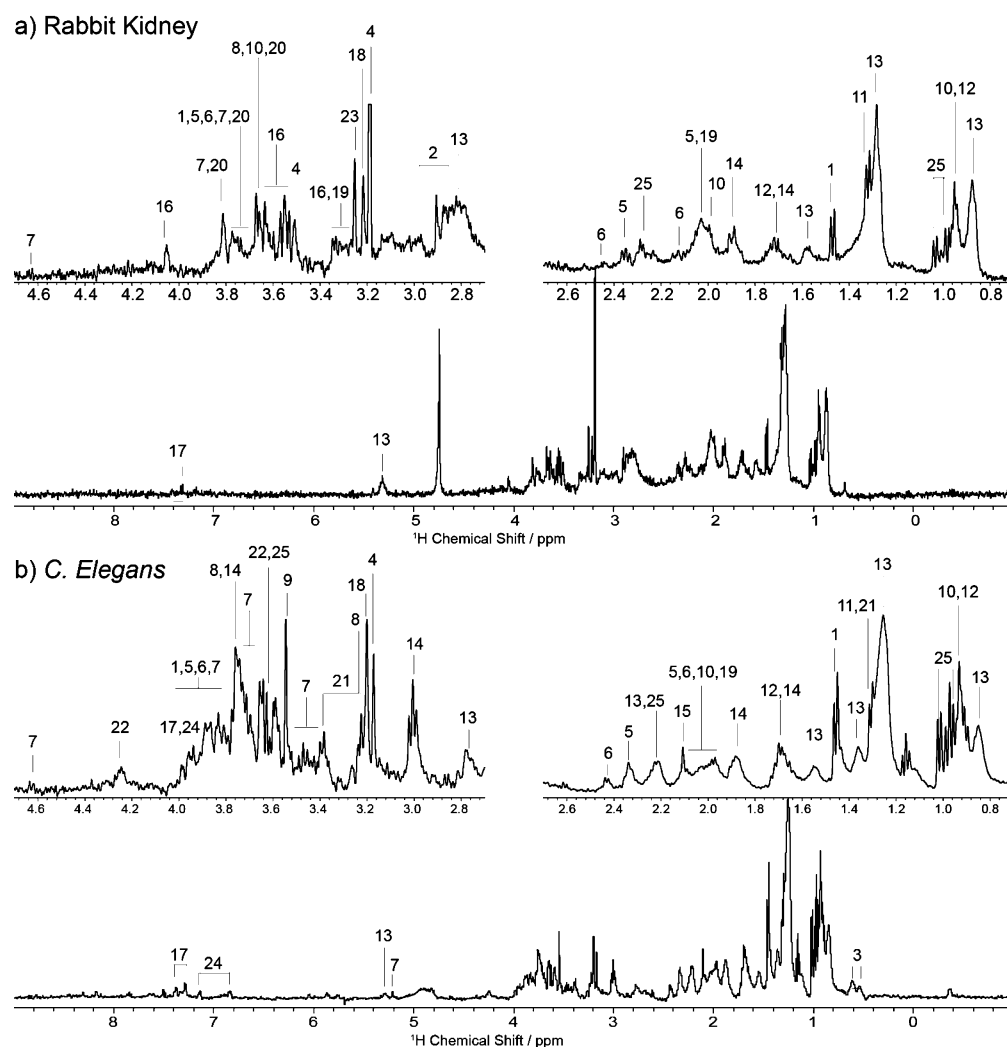


Figure 4. ^1H 2D-PASS HR-MACS spectra at 11.75 T of about 250 nL (a) rabbit kidney tissue and (b) *Caenorhabditis elegans* nematodes. The 2D-PASS spectra were acquired with two and one rotor-synchronized periods, respectively. Spectra are processed with LB = 0.2 Hz exponential apodization. The assignments 1–25 are the identified metabolites in the samples (see Table 1).

sample size. Consequently, a poorly resolved doublet is observed owing to the temperature-dependent resonance frequency shift.

Unfortunately, compared to Shapal-M (80 W/Km), Kel-F does not have good thermal conductivity (0.21 W/Km) for dissipating the heat generated from the coil by the eddy currents. The Kel-F insert adopted here is to optimize the spectral resolution under slow MAS conditions and not for fast MAS experiments. Ideally, isotropic susceptibility materials with high thermal conductivity would be a favorable choice for the inserts. It allows for faster MAS acquisitions while maintaining the high-resolution performance with better sensitivity compared to slow MAS. This is because under slow MAS the intensity of the isotropic resonances is distributed to its spinning sidebands; as a result, it reduces the isotropic intensity. Nonetheless, the spinning-sideband manifolds would be small for semisolid samples like biopsies.

HR-MACS NMR Spectroscopy of Nanoliter Tissues.

Figure 4 displays the high spectral quality of two different nanoliter (250 nL) tissues obtained from the refined HR-MACS resonator: (a) rabbit kidney tissue spinning at 433 Hz with a total experimental time of 3.1 h and (b) *Caenorhabditis elegans* nematodes spinning at 385 Hz with a recording time of

48 min. The high spectral resolution capable from HR-MACS allows resolution of many well-defined resonances including J-splitting such as the doublets of valine at 0.97 and 1.02 ppm with $^3J_{\text{H-H}} = 7.7$ and 7.2 Hz, respectively, lactate at 1.33 ppm with 7.1 Hz, and alanine at 1.47 ppm with 7.9 Hz. Furthermore, owing to the sensitivity enhancement, the spectra also reveal weak resonances of the aromatic protons in phenylalanine and tyrosine at 7–8 ppm. These enhanced resolution and sensitivity spectra render an in-depth metabolic profiling; a total of 25 metabolites have been identified (Table 2) from both spectra. This would not be possible with the nonrefined MACS resonator.⁴ Besides the resolution, the enhanced sensitivity (6.7-fold for the kidney tissue and 6 for the nematode) also plays a crucial role for the NMR experiments of the delicate samples. It allows acquisition of good quality spectra in reasonable time spans. Without HR-MACS, it would require 45 and 36 times, respectively, longer for the NMR acquisition in order to obtain spectra with the same signal-to-noise shown in Figure 4.

The slow MAS experiment performed here not only minimized the eddy current effects on the line width described above, but also reduced the centrifugal force ($F = m\omega_r^2 r_s$, where m and r_s are the sample mass and radius, respectively) exerted

Table 2. ^1H Chemical Shift Assignments of Rabbit Kidney and *Caenorhabditis elegans* from Figure 4

code	metabolite ^a	^1H shift (multiplicity) ^b
1	alanine	1.47(d), 3.77(m)
2	asparagine	2.84(dd), 2.94(dd)
3	cholesterol	0.54(m), 0.61(m)
4	choline	3.19(s), 3.50(m)
5	glutamate	2.05(m), 2.36(dt), 3.76(m)
6	glutamine	2.13(m), 2.43(m), 3.76(m)
7	α -glucose	3.42(m), 3.55(t), 3.76(m), 3.81(m), 3.92(m), 5.23(d)
	β -glucose	3.41(dd), 3.47(dd), 3.92(m), 4.61(d)
8	GPC	3.24(s), 3.67(dd), 3.78(m)
9	glycine	3.56(s)
10	isoleucine	0.91(t), 0.99(d), 1.96(m), 3.65(m)
11	lactate	1.33(d)
12	leucine	0.94(d), 0.96(d), 1.66(m), 1.70(m)
13	lipids	0.87(m), 1.12(m), 1.27(m), 1.36(m), 1.58(m), 2.26(m), 2.79(m), 5.31(m)
14	lysine	1.47(m), 1.70(m), 1.90(m), 3.02(t), 3.75(t)
15	methionine	2.13(s)
16	myo-inositol	3.28(m), 3.53(m), 3.62(m), 4.06(t)
17	phenylalanine	3.98(dd), 7.32(m), 7.40(m)
18	phosphorylcholine	3.22(s)
19	proline	2.05(m), 3.36(m)
20	sorbitol	3.66(m), 3.77(m), 3.82(m)
21	taurine	3.23(t), 3.38(t)
22	threonine	1.32(d), 3.59(m), 4.26(m)
23	TMAO	3.25(s)
24	tyrosine	6.87(d), 7.17(d)
25	valine	0.97(d), 1.02(d), 2.28(m), 3.61(d)

^aGPC = glycerophosphocholine; TMAO = trimethylamine-*N*-oxide.

^bThe assignments are based on refs 17–19. Abbreviations: s = singlet; d = doublet; dd = doublet of doublets; t = triplet; m = multiplet.

upon the sample.^{3,16} This is especially important for delicate samples. For example, in the case of the HR-MACS detection of the *Caenorhabditis elegans* nematodes, the force is small and negligible, 0.0004 N, whereas a much larger force of 15 N is experienced by the nematodes using the bulk sample HR-MAS detection with 30 μL of sample spinning at 3500 Hz.¹⁷ Furthermore, the excellent spectral quality shown in the figure suggests that even with slow sample spinning at magic-angle it is efficient to average out the heterogeneous susceptibility inside the tissues. Similar observations have also been reported by Wind and Hu.¹⁶ The results here clearly illustrate the superior detection quality in both resolution and sensitivity from the HR-MACS resonator for metabolic analyses of nanoliter biopsies.

This demonstrative study shows that eliminating the sample heating from the eddy currents in a spinning microcoil and any anisotropic magnetic susceptibility materials in close proximity to the sample could dramatically improve the spectral resolution, while maintaining a good sensitivity level for nanoliter MAS NMR detections. These results are valuable criteria for designing microfabrication of rotating resonators for high quality magnetic resonance studies using automated and reproducible techniques such as wire-bonding²⁰ or lithography.²¹ With the advances in microtechnologies, we anticipate that HR-MACS could be a vital magnetic resonance microprobe for noninvasive fine-needle biopsies of scarce human tissues and could potentially be implemented in clinical metabolic phenotyping.²²

AUTHOR INFORMATION

Corresponding Author

*Tel: +33 1 69 08 41 05. Fax: +33 1 69 08 66 40. E-mail: alan.wong@cea.fr.

Present Address

[§]Chinese Academy of Sciences, Institute of Electrical Engineering, 6 Beiertiao, Zhongguancun, 100190, Beijing, China.

Notes

The authors declare no competing financial interest.

ACKNOWLEDGMENTS

We would like to thank Dr. Jacques-François Jacquinot (CEA, France) for the stimulating discussions and assistance on the thermal simulations, Dr. Bénédicte Elena-Herrmann (CRMN, France) for providing the *C. elegans* samples, Dr. Beatriz Jiménez (Imperial, England) for her discussions on NMR-based biopsy studies, Dr. Pedro Aguiar (University of York, England) for his comments on the manuscript, and Mr. Angelo Guiga (CEA, France) for machining the inserts. The research leading to these results has received funding from the European Research Council under the European Community's Seventh Framework Programme (FP7/2007-2013), ERC Grant agreement 205119.

REFERENCES

- (1) Sakellariou, D.; Le Goff, G.; Jacquinot, J.-F. *Nature* **2007**, *447*, 694–697.
- (2) Jacquinot, J.-F.; Sakellariou, D. *Concepts Magn. Reson., Part A* **2011**, *38*, 33–51.
- (3) Wong, A.; Aguiar, P. M.; Sakellariou, D. *Magn. Reson. Med.* **2010**, *63*, 269–274.
- (4) Wong, A.; Jiménez, B.; Li, X.; Holmes, E.; Nicholson, J. K.; Lindon, J. C.; Sakellariou, D. *Anal. Chem.* **2012**, *84*, 3843–3848.
- (5) Beckonert, O.; Coen, M.; Keun, H. C.; Wang, Y.; Ebbels, T. M. D.; Holmes, E.; Lindon, J. C.; Nicholson, J. K. *Nature* **2010**, *5*, 1019–1032.
- (6) Doty, F. D.; Entzminger, G.; Yang, Y. A. *Concepts Magn. Reson.* **1998**, *10*, 239–260.
- (7) Piotto, M.; Elbayed, K.; Wieruszkeski, J.-M.; Lippens, G. *J. Magn. Reson.* **2005**, *173*, 84–89.
- (8) Sodickson, A.; Cory, D. G. *J. Magn. Reson.* **1997**, *128*, 87–91.
- (9) Antzutkin, O. N.; Shekar, S. C.; Levitt, M. H. *J. Magn. Reson. A* **1995**, *115*, 7–19.
- (10) van Gorkum, L. C. M.; Hook, J. M.; Logan, M. B.; Hanna, J. V.; Wasylishen, R. E. *Magn. Reson. Chem.* **1995**, *33*, 791–795.
- (11) Stringer, J. A.; Bronnimann, C. E.; Mullen, C. G.; Zhou, D. H. H.; Stellfox, S. A.; Li, Y.; Williams, E. H.; Rienstra, C. M. *J. Magn. Reson.* **2005**, *173*, 40–48.
- (12) Aguiar, P. M.; Jacquinot, J.-F.; Sakellariou, D. *J. Magn. Reson.* **2009**, *200*, 6–14.
- (13) Aubert, G.; Jacquinot, J.-F.; Sakellariou, D. *J. Chem. Phys.* **2012**, *137*, 154201.
- (14) Wishart, D. S.; Bigam, C. G.; Yao, J.; Abildgaard, F.; Dyson, H. J.; Oldfield, E.; Markley, J. L.; Sykes, B. D. *J. Biomol. NMR* **1995**, *6*, 135–140.
- (15) VanderHart, D. L. In *Encyclopedia of Nuclear Magnetic Resonance*; Grant, D. M., Harris, R. K., Eds.; Wiley: New York, 1996; Vol. 1, pp 2938–2946.
- (16) Wind, R. A.; Hu, J. Z. *Prog. Nucl. Magn. Reson. Spectrosc.* **2006**, *49*, 207–259.
- (17) Blaise, B. J.; Giacomotto, J.; Elena, B.; Dumas, M.-E.; Toulhoat, P.; Ségalat, L.; Emsley, L. *Proc. Nat. Acad. Sci.* **2007**, *104*, 19808–19812.
- (18) Garrod, S.; Humpfer, E.; Spraul, M.; Connor, S. C.; Polley, S.; Connelly, J.; Lindon, J. C.; Nicholson, J. K.; Holmes, E. *Magn. Reson. Med.* **1999**, *41*, 1108–1118.

- (19) Nicholson, J. K.; Foxall, P. J. D.; Spraul, M.; Farrant, R. D.; Lindon, J. C. *Anal. Chem.* **1995**, *67*, 793–811.
- (20) Badilita, V.; Fassbender, B.; Kratt, K.; Wong, A.; Bonhomme, C.; Sakellariou, D.; Korvink, J. G.; Wallrabe, U. *PLoS One* **2012**, *7*, No. e42848.
- (21) Malba, V.; Maxwell, R.; Evans, L. B.; Bernhardt, A. F.; Cosman, M.; Yan, K. *Biomed. Microdevices* **2003**, *5*, 21–27.
- (22) Nicholson, J. K.; Holmes, E.; Kinross, J. M.; Darzi, A. W.; Takats, Z.; Lindon, J. C. *Nature* **2012**, *491*, 384–392.